21st Annual Conference of the Canadian Nuclear Society
Toronto, Ontario, Canada / June 11 - 14, 2000

On relating inelastic and redistributed elastic analyses stress distributions

Prasad Mangalaramanan
Wolf Reinhardt

Babcock & Wilcox Canada, 581 Coronation Boulevard, Cambridge, Ontario
Canada N1R 5V3

Abstract

The classical lower bound theorem in plasticity states that the load required to create equilibrium stresses in a structure that are below yield will always be less than or equal to the collapse load. Recent advances in determination of lower bound limit loads involve repeated elastic analysis after systematic modification of elastic moduli. The intention is to obtain lower bound limit loads from stress fields that would progressively approach a state similar to one at plastic limit. The gradual transformation of statically admissible stress fields from elastic to limit state can be compared to various creep distributions corresponding to power-law creep indices ranging from one to infinity. This paper attempts to establish such one-to-one relation by using stress fields obtained from repeated elastic analyses.

1. Introduction

Limit analysis has been recognized by the ASME Code, Section III, NB-3228 [1] as one of the methods for designing pressure components. The advantage of limit analysis lies in the fact that it dispenses with conventional stress classification procedures and hence the uncertainty in designating whether a particular kind of stress is primary or secondary. Inelastic finite element analysis still remains as one of the reliable methods for determining limit loads, although closed form and lower bound solutions are available for simple configurations. Over the last decade, many researchers [2-5] have attempted to determine lower bound limit loads using stress fields based on linear elastic finite element analyses (LEFEA). These methods were premised on the fact that systematic modification of elastic moduli coupled with repeated elastic analyses would cause stress redistribution such that the value of maximum stress would be lower than the one during previous elastic analysis. It should be noted that any finite element stress field is statically admissible as long as the maximum equivalent stress is below the yield stress value. The structure by virtue of its geometry, loading and boundary conditions redistributes the stresses in a manner that is in tune with the nature of the structure. Application of these methods to a large number of isotropic component configurations demonstrated consistently good limit load estimates. Recently Mangalaramanan et. al [6] and, Reinhardt and Mangalaramanan [7] extended the modified moduli method for determining limit loads of orthotropic components and tubesheets. The limit load estimates compared well with those obtained using inelastic finite element analysis. Despite the success of the modified elastic moduli methods, no systematic study has thus far been performed for verifying whether changing elastic moduli does indeed redistribute the stress field in a manner conducive for obtaining better lower bound limit loads with progressive iterations. The question of quantifying the effect of elastic moduli change on the stress field obtained by subsequent elastic analysis has not been answered yet. This paper attempts to show the possibility of establishing a one-to-one correspondence between the stationary stress distributions obtained by power-law creep and those obtained by means of modified moduli method. Standard engineering problems considered to demonstrate this are a beam subjected to bending and a thick cylinder under internal pressure.

2. Pressure Component Design based on Stress Classification and Limit Analysis:

Knowledge of post-yield reserve strength of structures has drawn the attention of analysts over the past many decades. The ASME code also recognizes this aspect, thereby allowing designers to use limit analysis or elastic-plastic analysis as an alternative to conventional stress classification based component design [1]. Stress classification methods of pressure vessel design evolved during a time when finite element analysis and computing power were in their infancy. The idea of classifying stresses as membrane and bending based on free-body diagrams and beam on elastic foundation theory was elegant and offered conceptual insight on the problem, albeit being limited in scope of application. With advancement in computer hardware and software, commercial programs such as ANSYS [8] have implemented options for linearizing finite element stresses. However, there are many instances where the fundamental question of whether to classify a particular stress as primary stands to be debated [9]. The orientation of the stress class lines also becomes a deciding factor on the magnitude of finite element analysis based linearized stresses. There may be critical locations in components where it would be practically impossible to define a stress linearization path that would offer meaningful results (Figures 1 and 2). Conventional methods also do not account for the significant amount of post-yield reserve strength, especially in multiply redundant structures. Therefore the idea of determining limit loads and thereby coming up with the maximum possible design load as per ASME Code Section III, NB-3228 [1] offers advantages to designers in terms of cost savings and ease of analysis.

The downside of performing limit analysis, however, is the requirement of computer software that would be capable of performing non-linear analysis, the run-time and memory requirements. The advantage offered by ever increasing speed and memory of computers is somewhat offset by the inherent “desire” of the analyst to go for more detailed finite element models, higher order elements and finer mesh sizes. This on one side, non-linear analysis is still viewed with skepticism by “traditional” engineers, who feel more “at home” with stress classification procedures based on linear elastic analysis. The main reasons are because linear elastic finite element codes have been around for long, are easily bench marked and therefore chances of analysis errors are less. An independent limit analysis method based on LEFEA would therefore be an alternative at least for bench marking non-linear limit analysis results. Over the last decade, a number of researchers have endeavored to develop such procedures. Marriott [2], and Mackenzie et. al [4] have developed methods to determine limit loads using the classical lower bound limit load theorem. Lower bound limit loads are obtained by linearly scaling a set of LEFEA stress distributions such that the maximum von Mises equivalent stress is equal to the yield stress. Seshadri's [3] r-node method uses two LEFEA for determining reference stress [10] in components by identifying load-controlled locations called as redistribution nodes (r-nodes). The reference stress obtained using this method is linearly scaled to yield stress value for obtaining limit load. Since the aforementioned methods are based on well-established engineering concepts such as "classical lower bound theorem" and "reference stress," they not only offer the robustness of elastic analysis but also the advantage of limit analysis.

The methods described above attempt to produce redistributed stress fields by systematically modifying the elastic moduli. Artificially reducing the elastic properties of highly stressed regions (and vice-versa) ensures that these regions would be stressed less during the subsequent elastic analysis. The moduli modification method widely recognized as appropriate for stress redistribution is given by [3]:

$$E_s = E_o \left[\frac{\sigma_{arb}}{\sigma_{eqv}} \right] \tag{1}$$

where E_o is the original elastic modulus, σ_{arb} is some arbitrary stress value, σ_{eqv} is the von-Mises equivalent stress and E_s is the modified elastic modulus. The elastic modulus of every element is modified in inverse proportion to its equivalent stress and elastic analysis is subsequently performed. This results in stress redistribution which is akin (or at least that is what is intended) to what happens during inelastic analysis. The elastic stress fields obtained can be made to obey the stipulations of classical lower bound limit analysis. The limit load procedures based on the above theory were found to provide good limit load estimates [3-5]. Mackenzie et. al, have provided an exhaustive review of elastic modui modification procedures [11]. This paper attempts to quantify the behavior of elastic stress distribution consequent to moduli modification by establishing correspondence with power-law creep, for standard component configurations.

3. Limitations of Elastic Analysis Based Methods

The simplified limit analysis methods, however, have some limitations. Investigations [5] have revealed that modifying the elastic moduli and carrying out multiple linear elastic analyses need not necessarily redistribute the stress fields as in inelastic case. Sensitive structures such as non-symmetric plates and thin shells can exhibit poor convergence, as shown in Figures 3 and 4. Mangalaramanan and Seshadri [12] introduced an elastic moduli modification factor (EMMF) in an attempt to improve convergence. Using this procedure, the elastic moduli of an element, E, can be modified as follows:

$$E_s = E_o \left[\frac{\sigma_{arb}}{\sigma_{eqv}} \right]^q \qquad (2)$$

While a lower value of q effectively reduce the erratic fluctuations, it can increase the number of elastic analyses necessary to approach limit-state. It becomes important for an analyst to know the optimum value of q that would be necessary for smooth convergence to limit state and at the same time limit the number of iterations to some reasonable value. This, of course, depends on the type of problem analyzed.

While the difficulty in establishing a rational procedure for determining q before hand is accepted, it would be worthwhile to investigate whether the stress redistribution because of elastic analyses follows inelastic trend. The forthcoming sections investigate this aspect.

One other problem with repeated elastic iterations is that achieving a limit type of stress distribution may not always be possible. With a number of iterations, the difference between the maximum and minimum elastic moduli in a given elastic analysis can be large enough to render the elastic stiffness matrix ill conditioned.

4. Stress Redistribution in a Beam subjected to Pure Bending based on Elastic Moduli Modification Process:

A beam of rectangular cross-section and thickness t, subjected to pure bending as shown in Figure 5 is considered. The bending moment, M, in the beam can be expressed in terms of the equivalent stress as:

$$M = \int_{-t/2}^{t/2} \sigma z \, dz \qquad (3)$$

Throughout this paper, the superscripts *I, II, III,* … denote the first, second, third linear elastic analyses and so on. The equivalent stress, denoted by σ, in case of pure bending is the stress in axial direction.

4.1 First linear elastic analysis:

The stresses can be expressed in terms of the strains as $\sigma^I = \varepsilon^I E^I$, where the through thickness distribution of axial strain can be expressed in terms of the curvature as $\varepsilon^I = \kappa^I z$. Equation (3) can therefore be written as:

$$M = 2\int_{0}^{t/2} E^I \kappa^I z^2 dz = k^I E^I \frac{t^3}{6} \qquad (4)$$

Noting the relation between the stress, strain and curvature, the above equation becomes:

$$\sigma^I = \frac{Mz}{I} \qquad (5)$$

where the denominator I stands for the geometric moment of inertia.

4.2 Second linear elastic analysis:

The purpose of the second and subsequent linear elastic analyses is to redistribute the elastic stress fields in order to simulate the non-linear post-yield nature. This is achieved by systematically modifying the elastic moduli followed by an elastic analysis.

Since the bending moment is constant, it can be expressed in terms of the second elastic stress distribution as:

$$M = \int_{-t/2}^{+t/2} \sigma^{II} z dz \tag{6}$$

where $\sigma^{II} = E^{II} \varepsilon^{II}$, and $\varepsilon^{II} = k^{II} z$.

Therefore, the moment becomes

$$M = \int_{-t/2}^{+t/2} k^{II} E^{II} z^2 dz \tag{7}$$

The second elastic analysis elastic moduli, E^{II}, can be obtained from the first elastic analysis stress distribution as:

$$E^{II} = E^{I} \left[\frac{\sigma^{I}_{arb}}{\sigma^{I}} \right]^{q} \tag{8}$$

Substituting equations (5) and (8) into equation (7) and after performing the necessary integration, the curvature corresponding to the second elastic analysis is obtained as:

$$k^{II} = \frac{(3-q) M^{(q+1)}}{2 E^{I} \left(\sigma^{I}_{arb}\right)^{q} I^{q} \left[\frac{t}{2} \right]^{(3-q)}} \tag{9}$$

By invoking the stress-strain and strain-curvature relationships on equation (9), the stress distribution corresponding to second elastic analysis can be obtained as[1]:

$$\sigma^{II} = \frac{(3-q) z^{(1-q)} M}{2 \left[\frac{t}{2} \right]^{(3-q)}} \tag{10}$$

---

[1] Corollary:
Imposing $q = 1$, equation (10) becomes:

$$\sigma^{II} = \frac{4M}{t^2} \tag{F.1}$$

which is a constant through thickness stress distribution, independent of z, and hence limit type.

4.3 Third linear elastic analysis:

The moment equation for the third elastic analysis is given by:

$$M = \int_{-t/2}^{+t/2} k^{III} E^{III} z^2 dz \qquad (11)$$

The elastic moduli, E^{III}, can be obtained as follows:

$$E^{III} = E^{II} \left[\frac{\sigma_{arb}^{II}}{\sigma^{II}} \right]^r \qquad (12)$$

Substituting equation (8) in equation (12), we get

$$E^{III} = \frac{E^I \left[\sigma_{arb}^I I\right]^q \left[\sigma_{arb}^{II}\right]^r \left[2\left(\frac{t}{2}\right)^{(3-q)} \right]^r}{(3-q)^r M^{(q+r)} z^{q+r(1-q)}} \qquad (13)$$

which results in equation (11) to become:

$$M = \int_{-t/2}^{+t/2} \frac{k^{III} E^I \left[\sigma_{arb}^I I\right]^q \left[\sigma_{arb}^{II}\right]^r \left[2(t/2)^{(3-q)}\right]^r}{(3-q)^r M^{(q+r)} z^{q+r(1-q)}} z^2 dz \qquad (14)$$

The radius of curvature, k^{III}, can be obtained by integrating equation (14):

$$k^{III} = \frac{M^{q+r+1} (3-q)^r \left[3-q+r(1-q)\right]}{2E^I \left[\sigma_{arb}^I I\right]^q \left[\sigma_{arb}^{II}\right]^r \left[2(t/2)^{(3-q)}\right]^r \left[t/2\right]^{[3-q+r(1-q)]}} \qquad (15)$$

Since $\varepsilon^{III} = k^{III} z$, and $\sigma^{III} = E^{III} \varepsilon^{III}$, the expression for stress can be derived from equation (15) as:

$$\sigma^{III} = \frac{\left[2+(1-q)(1-r)\right] z^{(1-q)(1-r)}}{2(t/2)^{[2+(1-q)(1-r)]}} M \qquad (16)$$

The results obtained from equations (5), (10) and (16) can be summarized as follows:

$$\sigma^I = M \left[\frac{2+(1)}{2\left(\frac{t}{2}\right)^{[2+(1)]}} \right] z \qquad (5)$$

$$\sigma^{II} = M\left[\frac{2+(1-q)}{2\left(\frac{t}{2}\right)^{[2+(1-q)]}}\right]z^{(1-q)} \tag{10}$$

$$\sigma^{III} = M\left[\frac{2+(1-q)(1-r)}{2\left(\frac{t}{2}\right)^{[2+(1-q)(1-r)]}}\right]z^{(1-q)(1-r)} \tag{16}$$

and by induction

$$\sigma^{IV} = M\left[\frac{2+(1-q)(1-r)(1-s)}{2\left(\frac{t}{2}\right)^{[2+(1-q)(1-r)(1-s)]}}\right]z^{(1-q)(1-r)(1-s)} \tag{17}$$

$$\vdots$$

and so on.

4.4. Relation between moduli modification and power-law creep for the beam

The stress-strain rate relationship postulated by power-law creep is of the form

$$\dot{\varepsilon} = B\sigma^{n} \tag{18}$$

In the above equation, $n = 1$ corresponds to linear elasticity and $n \to \infty$ corresponds to perfect plasticity. Since it is known from equation (10) that $q = 0$ corresponds to linear elasticity and $q = 1$ corresponds to perfect plasticity, a relationship between q and n can be established as:

$$q = 1 - \frac{1}{n} \tag{19}$$

Substituting equation (19) into equation (10) leads to:

$$\sigma^{II} = \left[\frac{2n+1}{3n}\right]\left[\frac{2z}{t}\right]^{\frac{1}{n}}\sigma_{\max} \tag{20}$$

The term $\sigma_{\max}$ is the maximum stress corresponding to the first linear elastic analysis. Equation (20) is the same as the one available in standard textbooks for stationary stress distributions based on power-law creep (page 23 of reference [13]).

4.5 Effect of Transverse Shear

The type of loading considered in the aforementioned discussions was pure bending. However, transverse loading and multiple plastic zones commonly occur in real life structures and is therefore of practical importance. The tendency of transverse shear is to cause the moment to vary along the neutral axis of the beam. For the case of pure bending, the moment is constant across the neutral axis and hence the stress distribution given by equation (F.1) is one at limit. However, this is not true for problems with transverse loading. The second linear elastic analysis can result in an equivalent stress distribution that is uniform across the thickness for dominant bending, but may not necessarily be one at limit. Additional elastic analyses are required to cause the stresses to redistribute along the neutral axis. Unlike in pure bending, the stress distribution is no longer uniaxial because of the presence of shear. The von Mises equivalent stress therefore becomes:

$$\sigma_e = \sqrt{\sigma_x^2 + 3\tau_{xy}^2} \tag{21}$$

For net section collapse,

$$\sigma_e = \sigma_Y \tag{22}$$

where σ_Y is the yield strength of the material. For dominant bending since the magnitude of shear is negligible as compared to the normal stress, equations (5), (10), (16) and (17) are assumed to hold good. It would be of interest to study the change in shear stress distribution with repeated elastic analyses. The force required to cause shear stress in a small element of the beam (Figure 6) can be expressed as:

$$\Delta F = \int_{z_1}^{t/2} \Delta\sigma dA \tag{23}$$

where $dA = dz$ for unit width of the beam. Equation (23) is available in all standard text books in engineering mechanics [14]. The factor $\Delta\sigma$ can be obtained from any of the equations (5), (10), (16) and (17). For the sake of illustration equation (10) is considered:

$$\Delta\sigma = \frac{(3-q)z^{(1-q)}\Delta M}{2\left[\frac{t}{2}\right]^{(3-q)}} \tag{24}$$

This results in equation (23) to become

$$\Delta F = \frac{(3-q)\Delta M}{2\left[\frac{t}{2}\right]^{(3-q)}} \int_{z_1}^{t/2} z^{(1-q)} dz \tag{25}$$

The shear stress can be determined from equation (25) as

$$\tau_{xy} = \lim_{\Delta x \to 0} \frac{\Delta F}{\Delta x} = \frac{3-q}{2\left[\frac{t}{2}\right]^{(3-q)}(2-q)} \left[\lim_{\Delta x \to 0} \frac{\Delta M}{\Delta x}\right] \left[\left(\frac{t}{2}\right)^{(2-q)} - z_1^{(2-q)}\right] \tag{26}$$

for $0 \le z_1 \le \frac{t}{2}$.

Equation (26) can be rewritten as[2]:

$$\tau_{xy} = \frac{(3-q)V}{2(2-q)\left[\frac{t}{2}\right]^{(3-q)}} \left[\left(\frac{t}{2}\right)^{(2-q)} - z_1^{(2-q)}\right] \tag{27}$$

where V is the shear force. Equation (19) can be applied on equation (27) for obtaining the shear stress in terms of power-law creep index.

---

[2] Corollary:

When $q = 0$, we get the well-known parabolic shear stress distribution given by

$$\tau_{xy}^{I} = \frac{6V}{t^3}\left[\left(\frac{t}{2}\right)^2 - z_1^2\right]$$

Substituting $q = 1$ leads to a linear limit shear distribution given by

$$\tau_{xy}^{II} = \frac{4V}{t^2}\left[\frac{t}{2} - z_1\right]$$

In situations where shear is dominant, assumption of a constant through thickness axial stress postulated by equation (F.1) violates the necessary condition given by equation (22). Equations (10), (15), (16) and (27) no longer hold good as there is no assurance that $q=1$ in equation (10) would lead to limit type stress distribution. Figure 7 shows the effect of the value of q on the stress distributions in the beam. The figure indicates that problems involving significant shear require a value of $q<1$ for good lower bound limit loads. Two numerical examples are considered in order to study the effect of transverse shear.

A rectangular plate partially fixed and partially simply supported, as shown in Figure 3, is considered to analyze the effect of shear. The configuration is chosen for studying the dominant shear effect. The Young's modulus and the yield strength of the material are assumed as 30000 ksi and 30000 psi, respectively. The problem is analyzed for two values of Poisson's ratio (ν=0.3 and 0.49) and two values of elastic moduli modification factors (q=0.25 and 1). The lower bound limit loads due to elastic iterations and inelastic limit load are also shown in Figure 3. It can be seen that the elastic moduli modification factor of q=1 leads to severe oscillations in the limit load estimates. However, using q=0.25 shows good convergence characteristics.

The next problem considered is a barrel shaped beam fixed on both ends and subjected to uniform pressure. The Young's modulus and yield stress values are the same as for the previous case. This problem has been chosen to demonstrate that while the second linear elastic analysis causes a uniform through thickness stress redistribution, subsequent elastic analyses are necessary for redistribution along neutral axis. The component configuration and the stress distributions are shown in Figure 8.

5. Stress Redistribution in a Cylinder subjected to Uniform Internal Pressure under Plane Strain Conditions

A cylinder of internal and external radii of r_i and r_o, respectively, as shown in Figure 9 is considered. The cylinder is subjected to uniform internal pressure, p, and is assumed to be long enough for plane strain conditions to hold good. The following equations apply:

The von Mises equivalent stress is given by:

$$\sigma_e = \frac{1}{\sqrt{2}}\left[(\sigma_r - \sigma_\theta)^2 - (\sigma_\theta - \sigma_z)^2 - (\sigma_z - \sigma_r)^2\right]^{\frac{1}{2}} \tag{28}$$

where σ_r, σ_θ and σ_z are respectively the radial, hoop and axial stresses.

Postulation of plane strain condition leads to the following relationship between the stress components:

$$\sigma_z = \frac{1}{\nu}(\sigma_r + \sigma_\theta) \tag{29}$$

Equation (29) and the assumption of plastic incompressibility ($\nu = 1/2$) reduces equation (28) to:

$$\sigma_e = \frac{\sqrt{3}}{2}(\sigma_\theta - \sigma_r) \tag{30}$$

The expression for equivalent strain can be obtained from standard text books (reference [10], page 50, equation 3.1a) as:

$$\varepsilon_e = \frac{2}{\sqrt{3}}\frac{C_1}{r^2} \qquad r_i \le r \le r_o \tag{31}$$

5.1 First linear elastic analysis

The stress-strain relationship is expressed as:

$$\sigma_e^I = E^I \varepsilon_e^I \tag{32}$$

Substituting equations (30) and (31) in (32), the following relation is obtained:

$$\sigma_\theta^I - \sigma_r^I = \frac{4}{3} E^I \frac{C_1}{r^2} \tag{33}$$

The equilibrium equation for a thick cylinder is given by:

$$\frac{d\sigma_r}{dr} = \frac{\sigma_\theta - \sigma_r}{r} \tag{34}$$

Equation (33) can be substituted into equation (34) leading to

$$\frac{d\sigma_r^I}{dr} = \frac{4}{3} E^I \frac{C_1}{r^2} \tag{35}$$

Integration of equation (35) gives the radial stress

$$\sigma_r^I = \frac{-2}{3} \frac{E^I C_1}{r^2} + C_2 \tag{36}$$

The following boundary conditions apply:

$$\text{at} \quad r = r_i; \quad \sigma_r^I = -p$$

$$r = r_o; \quad \sigma_r^I = 0 \tag{37}$$

resulting in $C_1 = \frac{3p}{2E^I} \frac{r_i^2 r_o^2}{r_o^2 - r_i^2}$.

The equivalent stress can be calculated from equations (30), (34), (35) and C_1 as[3]:

$$\sigma_e^I = \frac{\sqrt{3}p}{r^2} \frac{r_i^2 r_o^2}{r_o^2 - r_i^2} \tag{38}$$

5.2 Second linear elastic analysis

The stress-strain relationship corresponding to the second linear elastic analysis

$$\sigma_e^{II} = E^{II} \varepsilon_e^{II} \tag{39}$$

can be simplified as:

$$\sigma_\theta^{II} - \sigma_r^{II} = \frac{4}{3} E^{II} \frac{C_1}{r^2} \tag{40}$$

---

[3] Corollary:

σ_e^I is maximum at $r = r_i$. Therefore, $\left(\sigma_e^I\right)_{\max} = \frac{\sqrt{3} p r_o^2}{r_o^2 - r_i^2}$.

The second linear elastic analysis moduli is defined as follows:

$$E^{II} = E^{I}\left[\frac{\sigma^{I}_{arb}}{\sigma^{I}_{e}}\right]^{q} \tag{41}$$

From equations (30) and (38),

$$E^{II} = E^{I}\left[\frac{1}{\sqrt{3}}\sigma^{I}_{arb}\frac{r_o^2 - r_i^2}{-pr_o^2 r_i^2}\right]^{q} r^{2q} \tag{42}$$

which, for the sake of simplicity, can be expressed as

$$E^{II} = \mathrm{K} r^{2q} \tag{43}$$

Equation (43) is substituted in equation (40), leading to

$$\sigma^{II}_{\theta} - \sigma^{II}_{r} = \frac{4}{3}\mathrm{K} C_1 r^{2(q-1)} \tag{44}$$

Equation (44) when substituted into equation (34) results in the following expression:

$$\frac{d\sigma^{II}_{r}}{dr} = \frac{4}{3}\mathrm{K} C_1 r^{2(q-1)-1} \tag{45}$$

The above equation is integrated for obtaining the radial stress:

$$\sigma^{II}_{r} = \frac{4}{3}\mathrm{K} C_1 \frac{r^{2q-2}}{q-2} + C_2 \tag{46}$$

The arbitrary constant is obtained by applying the boundary conditions given by equation (37), resulting in:

$$C_1 = \frac{3}{4}\frac{\left[2p(1-q)\right]}{\mathrm{K}}\frac{r_o^{2(1-q)} r_i^{2(1-q)}}{r_o^{2(1-q)} - r_i^{2(1-q)}} \tag{47}$$

From equations (30), (44) and (47) the expression for equivalent stress is evaluated[4]:

$$\sigma^{II}_{e} = \frac{\sqrt{3}p(1-q)}{r^{2(1-q)}}\frac{r_o^{2(1-q)} r_i^{2(1-q)}}{r_o^{2(1-q)} - r_i^{2(1-q)}} \tag{48}$$

---

[4] Corollary:

Just as in the case of the beam, substituting $q = 0$ in equation (48) leads to the linear elastic solution. When $q = 1$, the following equation (48) becomes

$$\lim_{q\to 1}\sigma^{II}_{e} = \lim_{q\to 1}\frac{\sqrt{3}p(1-q)}{r^{2(1-q)}}\frac{r_o^{2(1-q)} r_i^{2(1-q)}}{r_o^{2(1-q)} - r_i^{2(1-q)}} = \frac{\sqrt{3}p}{2\ln(r_o / r_i)} \tag{F.2}$$

using L'Hospital's rule. The above equation corresponds to limit stress distribution because when σ^{II}_{e} reaches the yield value, the applied pressure p would reach the collapse pressure.

5.3 Third linear elastic analysis

The stress-strain relationship for the third linear elastic analysis is given by

$$\sigma_e^{III} = E^{III} \varepsilon_e^{III} \tag{49}$$

which can be simplified using equation (30) as

$$\sigma_\theta^{III} - \sigma_r^{III} = \frac{4}{3} E^{III} \frac{C_1}{r^2} \tag{50}$$

The elastic modulus E^{III} is determined as follows

$$E^{III} = E^{II} \left[\frac{\sigma_{arb}^{II}}{\sigma_e^{II}} \right]^s \tag{51}$$

The second linear elastic analysis stress, σ_e^{II}, is obtained from equation (48) as

$$\sigma_e^{II} = \frac{\mathrm{K}_1}{r^{2(1-q)}} \tag{52}$$

where $\mathrm{K}_1 = \dfrac{\sqrt{3} p(1-q) r_o^{2(1-q)} r_i^{2(1-q)}}{r_o^{2(1-q)} - r_i^{2(1-q)}}$, and E^{II} is obtained from equation (43), which makes equation (51) as:

$$E^{III} = \mathrm{K}_2 r^{2(s-qs+q)} \tag{53}$$

where $\mathrm{K}_2 = \dfrac{\mathrm{K}\sigma_{arb}^s}{\mathrm{K}_1}$.

Equations (43) and (50) when substituted into equation (34) leads to

$$\frac{d\sigma_r^{III}}{dr} = \mathrm{K}_3 C_1 r^{-2(1-s)(1-q)-1} \tag{54}$$

where $\mathrm{K}_3 = \dfrac{4}{3} \mathrm{K}_2$.

Equation (54) when integrated results in

$$\sigma_r^{III} = \mathrm{K}_3 C_1 \frac{r^{-2(1-s)(1-q)}}{-2(1-s)(1-q)} + C_2 \tag{55}$$

The boundary conditions provided by equation (37) are invoked for determining the arbitrary constant C_1:

$$C_1 = \frac{2p(1-s)(1-q)}{\mathrm{K}_3} \frac{r_o^{2(1-s)(1-q)} r_i^{2(1-s)(1-q)}}{r_o^{2(1-s)(1-q)} - r_i^{2(1-s)(1-q)}} \tag{56}$$

Equation (56) is substituted into equation (50) and the equivalent stress is obtained from equation (30) as:

$$\sigma_e^{III} = \frac{\sqrt{3}p(1-s)(1-q)}{r^{2(1-s)(1-q)}} \frac{r_o^{2(1-s)(1-q)} r_i^{2(1-s)(1-q)}}{r_o^{2(1-s)(1-q)} - r_i^{2(1-s)(1-q)}} \tag{57}$$

The results obtained from equations (38), (48) and (57) can be summarized as follows:

$$\sigma_e^{I} = \frac{\sqrt{3}p}{r^2} \frac{r_i^2 r_o^2}{r_o^2 - r_i^2} \tag{38}$$

$$\sigma_e^{II} = \frac{\sqrt{3}p(1-q)}{r^{2(1-q)}} \frac{r_o^{2(1-q)} r_i^{2(1-q)}}{r_o^{2(1-q)} - r_i^{2(1-q)}} \tag{48}$$

$$\sigma_e^{III} = \frac{\sqrt{3}p(1-s)(1-q)}{r^{2(1-s)(1-q)}} \frac{r_o^{2(1-s)(1-q)} r_i^{2(1-s)(1-q)}}{r_o^{2(1-s)(1-q)} - r_i^{2(1-s)(1-q)}} \tag{57}$$

and by induction

$$\sigma_e^{IV} = \frac{\sqrt{3}p(1-t)(1-s)(1-q)}{r^{2(1-t)(1-s)(1-q)}} \frac{r_i^{2(1-t)(1-s)(1-q)} r_o^{2(1-t)(1-s)(1-q)}}{r_o^{2(1-t)(1-s)(1-q)} - r_i^{2(1-t)(1-s)(1-q)}} \tag{58}$$

$$\vdots$$

and so on.

Whereas in the case of the beam the Poisson's ratio does not have any influence on equations (5), (10), (16) and (17), plastic incompressibility (ν=0.5) is assumed in deriving equations (38), (48), (57) and (58).

5.4. Relation between moduli modification and power-law creep for the cylinder

The same argument as in the case of the beam holds good in relating the elastic moduli modification index and the power-law creep index. Substituting equation (19) into equation (48) leads to:

$$\sigma_e^{II} = \frac{\sqrt{3}}{n}\frac{p}{r^{2/n}}\frac{r_i^{2/n} r_o^{2/n}}{r_o^{2/n} - r_i^{2/n}} \tag{59}$$

Equation (59) is the same as the stationary creep stress distributions available in standard textbooks (equation 3.2 in page 51 of reference [10]).

5.5 Shell structures forming multiple plastic hinges before collapse

Equation (F.2) points to the fact that the second linear elastic analysis produces limit distribution for a cylinder for q=1. The pressure components that one would commonly come across are usually of thin-shell type and form multiple plastic hinges at collapse. Such structures require more than two linear elastic iterations to account for the meridional, apart from the through-thickness, stress redistribution. An example of a torispherical head subjected to uniform internal pressure is considered. The Young's modulus and the yield strength of the material are assumed as 30000 ksi and 30000 psi, respectively. The problem is analyzed for two values of Poisson's ratio (ν=0.3 and 0.49) and three values of elastic moduli modification factors (q=0.25, 0.5 and 1). The lower bound limit loads due to elastic iterations and inelastic limit load are shown in Figure 4.

It can be seen that q=1 causes substantial oscillations in the limit load estimates while q=0.25 results in a much smoother limit loads convergence. This can be explained as follows. The pressure vessel configuration considered is thin-walled with dominant membrane action. The variation of stresses across such a thin section is not considerable. The inelastic stress redistribution is predominantly trans-meridional. The second linear elastic analysis for q=1 obviously results in a uniform through thinkness stress redistribution which is, however, not limit type. The trans-meridional stress redistribution requires a number of elastic iterations. However, imposing a q value of unity forces overmodification of elastic moduli value resulting in abnormal displacements in the structure. In order to obtain a limit type stress field, the strain fields must also approach limit type in accordance with the uniqueness theorem. The basis of moduli modification procedure is to progressively change the elastic properties in such a manner that the structure by itself decides the stress distribution for which it could maximize the internal energy, for a given traction. For thin structures such as torispherical head, a value of q=1 may be too abrupt to allow the gradual change.

6. Conclusion

This paper demonstrates the possibility of one-to-one correspondence between stress distributions based on power-law creep and those obtained from repeated elastic iterations. The examples of beam under bending and a cylinder subjected to uniform internal pressure show that the stress distributions obtained using moduli modification procedure are identical to the stationary distributions obtained by using creep power-law. Equations (5), (10), (16) and (17) for the beam and equations (38), (48), (57) and (58) for the cylinder have interesting implications. A value of EMMF of unity ensures that the subsequent elastic analysis would produce a limit distribution, thereby rendering additional analyses redundant. Also even an infinite number of elastic analyses for a moduli modification index less than unity cannot produce a limit type of stress distribution.

While the assumption of incompressibility necessitates that the Poisson's ratio should equal 0.5 for cylinder, it does not have any effect in the case of beam.

It has also been demonstrated that q=1 can cause difficulty in convergence of lower bound limit loads with elastic iterations. However, a smaller value of q, say q=0.25, can exhibit smoother convergence. The effect of transverse shear and formation of multiple hinges has also been investigated. A value of q between 0.25 and 0.5 is recommended for general pressure component design in order to reduce oscillations and ensure smooth convergence of lower bound limit loads.

References:

[1] ASME Boiler and Pressure Vessels Code, 1989, Section III, Division 1, Subsection NB-3000.

[2] Marriott, D.L., 1988, "Evaluation of Deformation or Load Control of Stresses under Inelastic Conditions using Elastic Finite Element Stress Analysis," Proceedings of the ASME-PVP Conference, Pittsburgh, Vol. 136.

[3] Seshadri, R., 1991, "The Generalized Local Stress Strain (GLOSS) Analysis – Theory and Applications," ASME Journal of Pressure Vessel Technology, Vol. 113, pp. 219-227.

[4] Mackenzie, D., and Boyle, J.T., 1993, "A Method for Estimating Limit Loads by Iterative Elastic Analysis. I-Simple Examples," International Journal of Pressure Vessels and Piping, Vol. 53, pp. 77-95.

[5] Seshadri, R., and Mangalaramanan, S.P., 1997, "Lower Bound Limit Loads using Variational Concepts: The m_α-method," International Journal of Pressure Vessels and Piping, Vol. 71, pp. 93-106.

[6] Mangalaramanan, S.P., Seshadri, R., and Reinhardt, W., 1999, "Limit Loads of Orthotropic Structures using the R-Node Method," Presented at the ASME Pressure Vessels and Piping Conference, Boston, Vol. 388.

[7] Reinhardt, W., and Mangalaramanan, S.P., 1999, "Efficient Tubesheet Design using Repeated Elastic Limit Analysis Technique," Proceedings of the ASME Pressure Vessel and Piping Conference, Vol. 385, pp. 141-149.

[8] ANSYS, 1997, ANSYS User's Manual for Revision 5.4, SAS IP Inc., Canonsburg, PA.

[9] Hollinger, G.L., and Hechmer, J.L., 1996, "Summary of Example Problems from PVRC Project on Three-dimensional Stress Criteria," Proceedings of the ASME Pressure Vessel and Piping Conference, Vol. 338, pp. 209-218.

[10] Kraus, H., 1980, Creep Analysis of Structures, Wiley-Interscience Publication.

[11] Mackenzie, D., Boyle, J.T., and Hamilton, R., 2000, "The Elastic Compensation Method for Limit and Shakedown Analysis: A Review," To Appear in Institute of Mechanical Engineers (IMechE) Journal.

[12] Mangalaramanan, S.P., and Seshadri, R., 1997, "Limit Loads of Layered Beams and Layered Cylindrical Shells using the R-Node Method," Presented in the ASME Pressure Vessels and Piping Conference, Orlando.

[13] Boyle, J.T., and Spence, J., 1983, Stress Analysis for Creep, Butterworths.

[14] Popov, E.P., 1976, Mechanics of Materials, Second Edition, Prentice-Hall Inc.

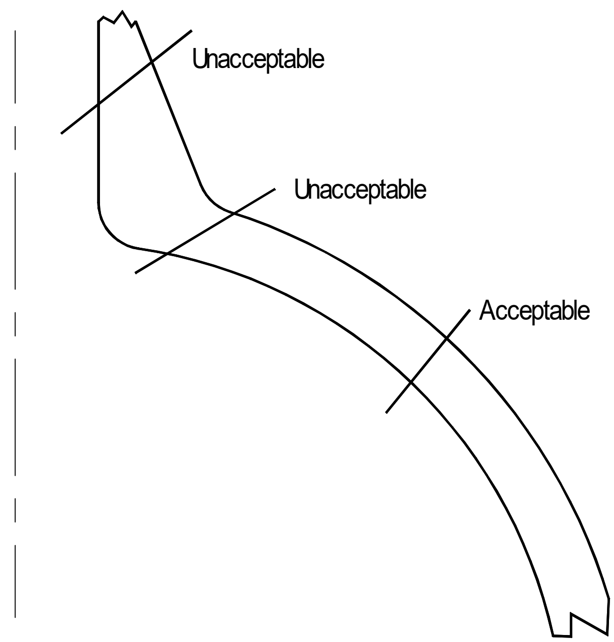

Figure 1: Acceptable and unacceptable orientations of stress classlines

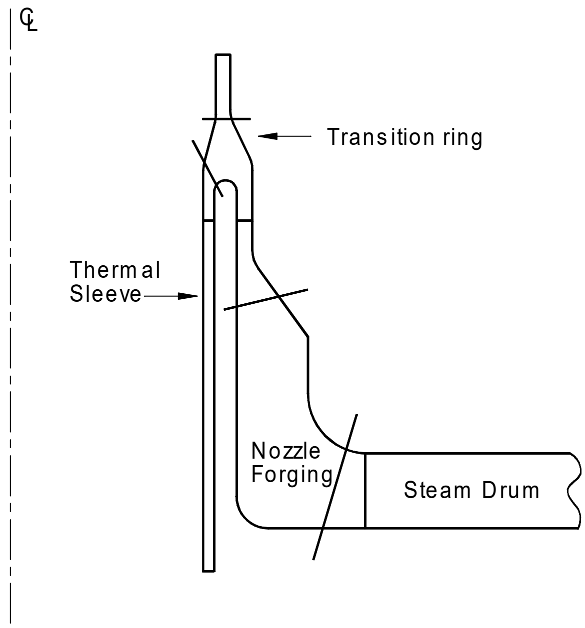

Figure 2: Critical locations in the feedwater nozzle of a steam generator where it is difficult to draw stress classlines

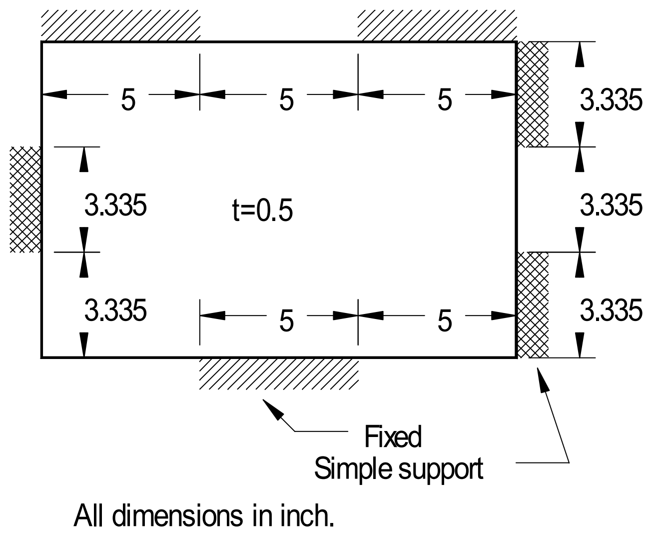

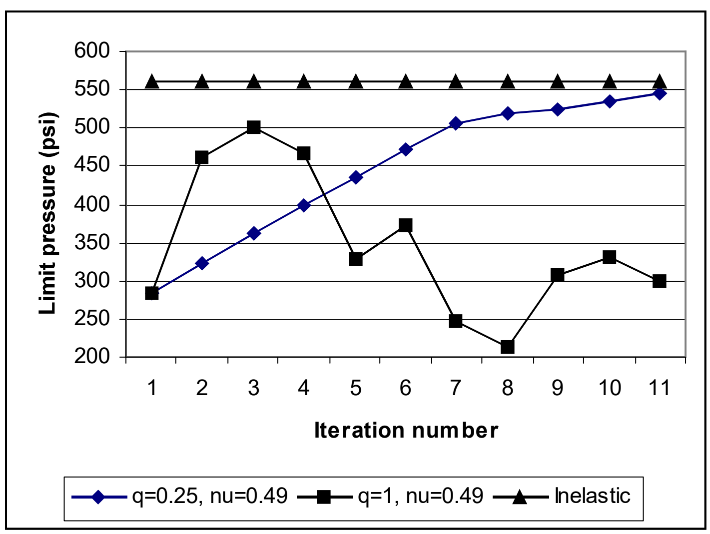

Figure 3: Non-symmetric rectangular plate and limit load estimates

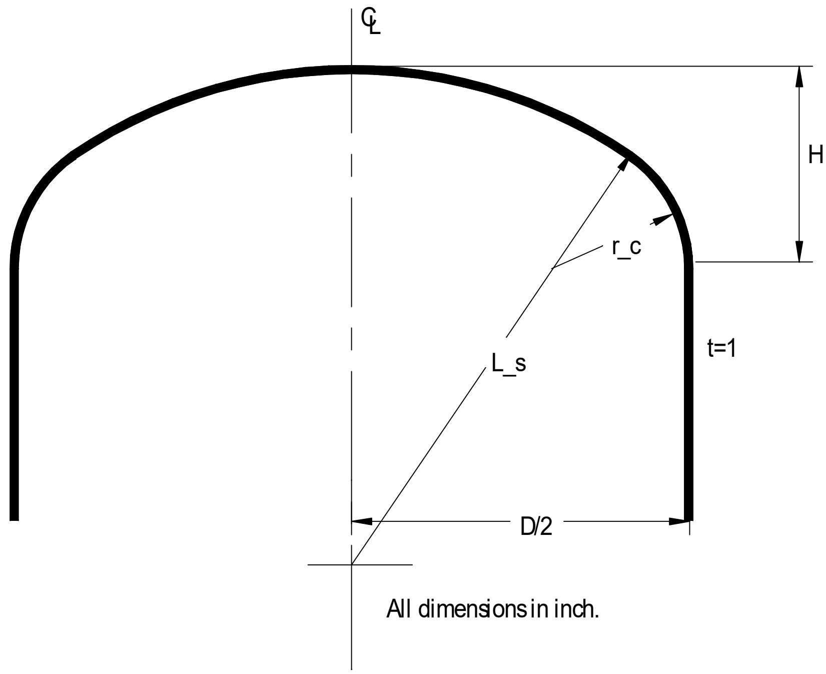

D/t=300 L_s/D=0.8 r_c/D=0.16 H/D=0.2577

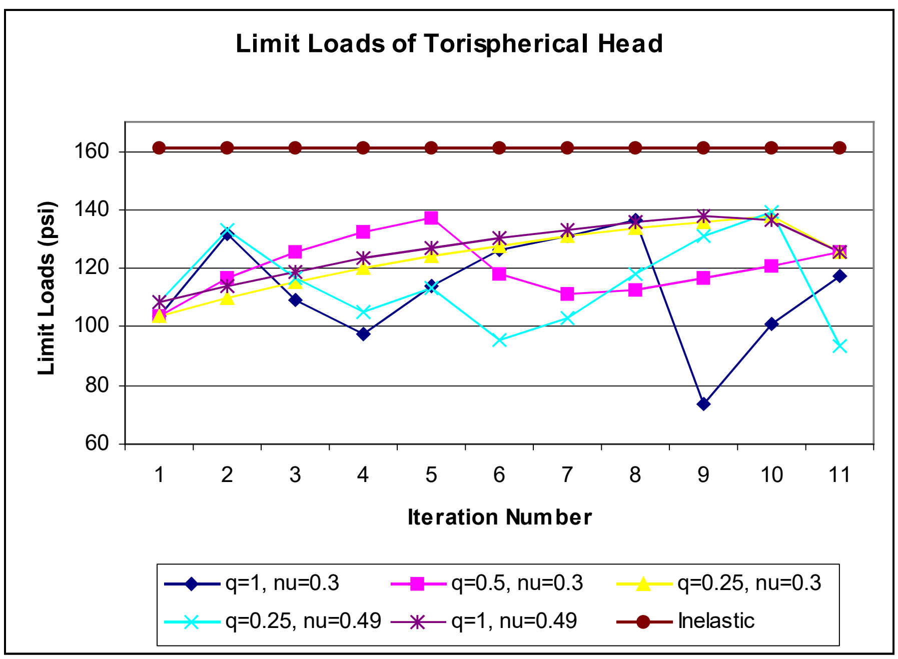

Figure 4: Torispherical head and limit load estimates

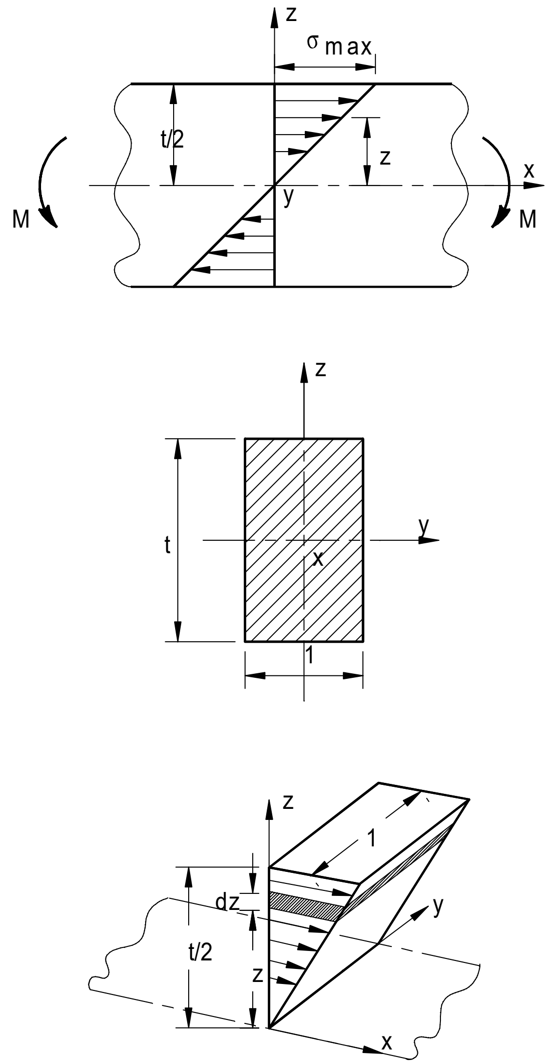

Figure 5: Rectangular beam subjected to bending

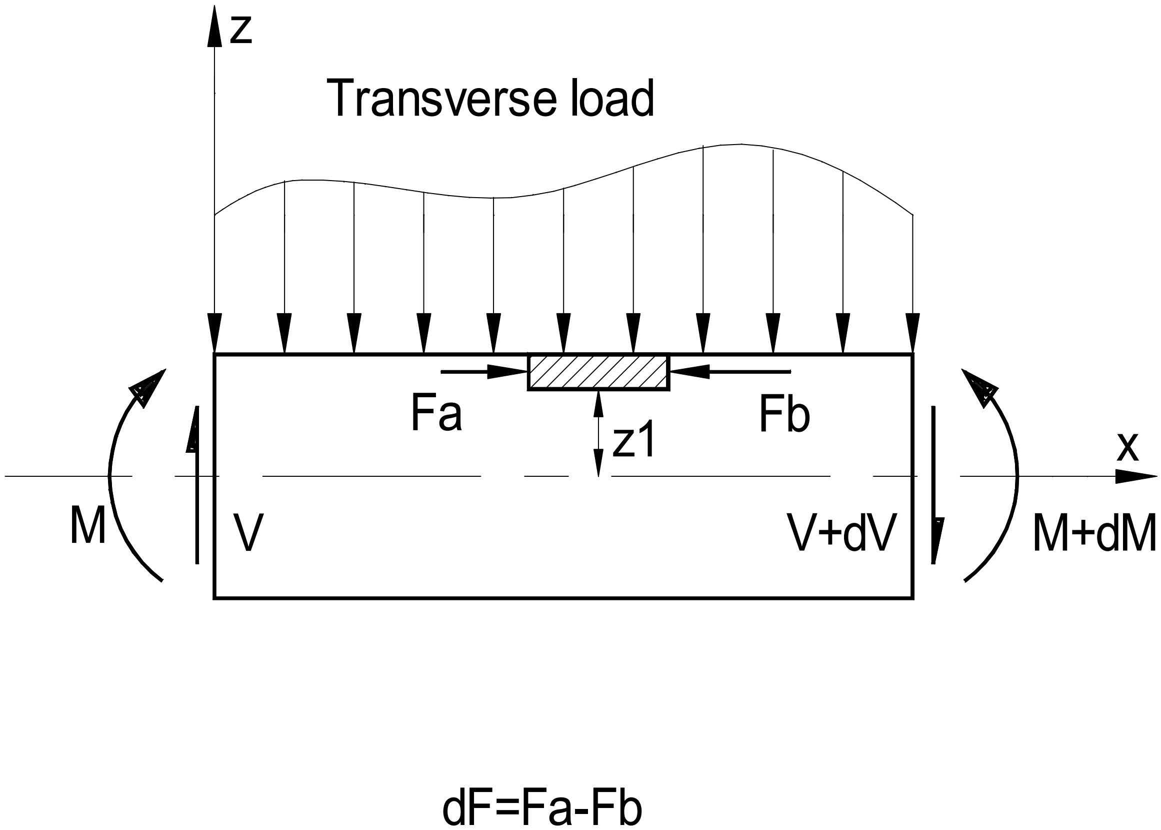

Figure 6: Transverse shear in beam

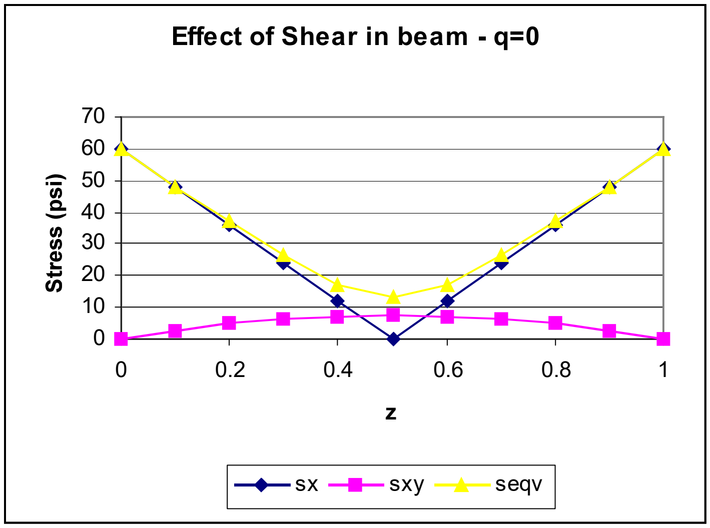

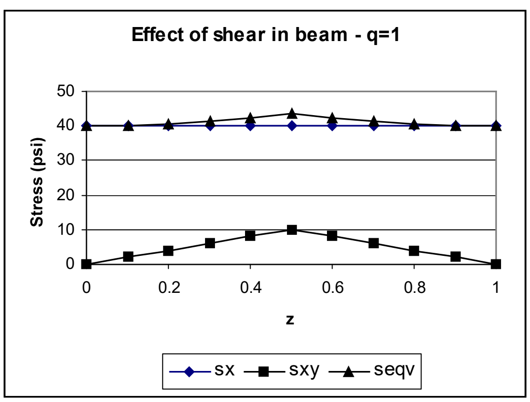

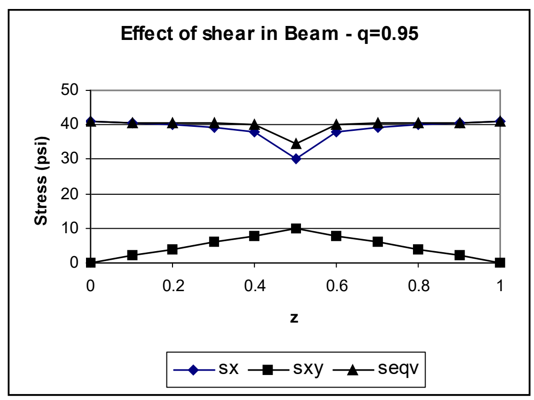

Moment = 10 lbf.in Shear force = 5 lbf Thickness = 1 inch

Normal, shear and equivalent stresses evaluated using equations (10), (27) and (21), respectively. In the above plots the absolute value of *sx* is used for the sake of clarity.

Figure 7: Effect of elastic moduli modification index on shear stresses in beam

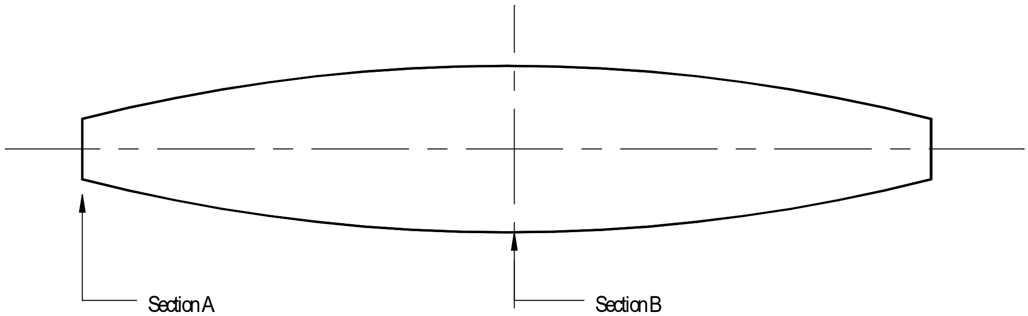

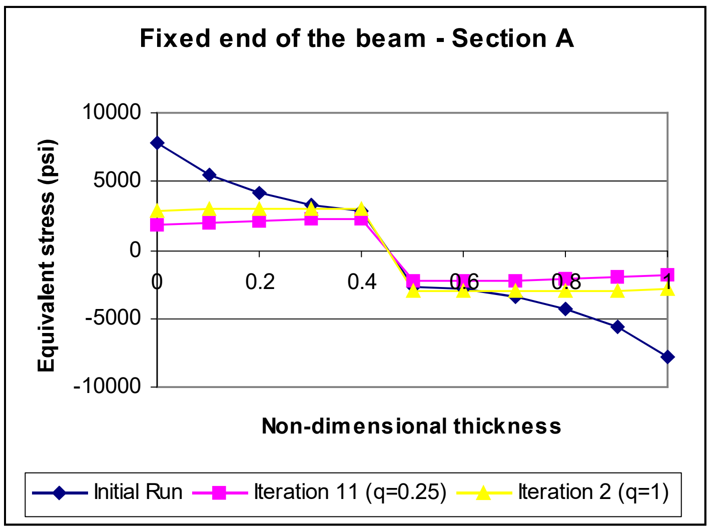

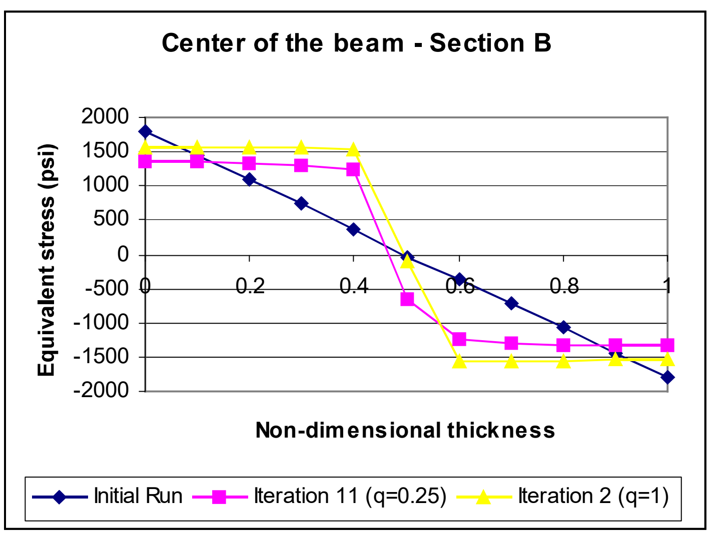

Note: In the above plots, the equivalent stress for the portions above the neutral axis is intentionally given negative sign in order to provide better visual interpretation.

Figure 8: Barrel shaped beam subjected to uniform pressure and stresses across the cross-section

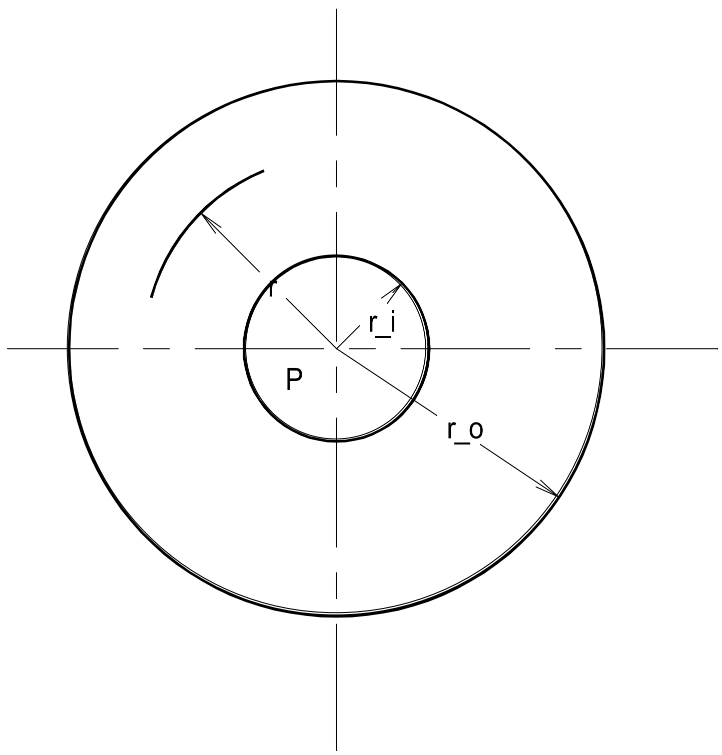

Figure 9: Cylinder under internal pressure